Studies of Emittance Growth in the ATF [1]

Frank Zimmermann

Stanford Linear Accelerator Center, Stanford, CA 94309

Abstract

Several different mechanisms of emittance growth in the Accelerator Test Facility (ATF) at KEK are investigated: I calculate rise times of the fast beam-ion instability for the damping ring (DR), and I discuss the emittance growth caused by coherent synchrotron radiation in the beam-transport line (BT), the effect of quadrupole wake fields in the injector linac, and, finally, a single-bunch head-tail ion effect that can occur in both the DR and the BT. A first attempt to measure the quadrupole wake on the real machine is also reported.

1 Introduction

The Accelerator Test Facility (ATF), currently being commissioned at KEK, consists of an S-band electron injector, a beam-transport line (BT), a damping ring (DR), an extraction line and (in the future) a bunch compressor and possibly an X-band linac. The ring is designed to produce a beam with normalized emittances of about $\gamma\epsilon_x \approx 4 \times 10^{-6}$ m rad and $\gamma\epsilon_y \approx 3 \times 10^{-8}$ m rad, as will be required for a next-generation linear collider. The alignment tolerances which have to be met to achieve this goal as well as the emittance growth from intra-beam scattering and from residual-gas scattering were discussed by Raubenheimer in Refs. [1] and [2].

In this paper, I will estimate the importance of other, more 'exotic' emittance-growth processes, which may be encountered as the ATF explores a new parameter regime. Specifically, I discuss

- the rise times of the multi-bunch fast beam-ion instability in the DR,

- single-bunch head-tail ion effects in the DR and the BT,

- single-bunch emittance growth caused by coherent synchrotron radiation in the BT, and

- the effect of quadrupole wake fields in the low-energy injector linac.

I will show that the first effect can be very severe: the fast beam-ion instability will impose a fairly tight tolerance on the vacuum pressure and could, in addition, require special countermeasures (such as a bunch-by-bunch orbit feedback or gaps in the bunch train). Also the quadrupole wake fields in the injector linac are shown to be potentially important. By contrast, both the head-tail ion effects and the emittance growth due to coherent synchrotron radiation are found to be insignificant.

DISCLAIMER

2 Emittance Growth in the Damping Ring

2.1 Fast Beam-Ion Instability

The fast beam-ion instability (FBII) is a single-pass effect, where an initial small perturbation grows exponentially due to the interaction of the electron-bunch train with residual-gas ions that are generated during the beam passage [3, 4, 5, 6, 7]. This instability, which was first predicted theoretically, has recently been observed in machine studies at the Advanced Light Source (ALS) [8] and at the Tristan Accumulation Ring [9]. In the ALS experiments, the vertical emittance at the end of the bunch train increased by a factor 2–4, when the vacuum pressure was elevated to ~50–100 ntorr by the controlled inflow of helium gas.

The FBII growth rate strongly depends on the number of bunches in the train, the transverse beam size, and the residual-gas pressure. Due to its small vertical emittance, large beam current, and fairly high pressure, the ATF is the only storage ring in operation which would allow us to study this instability in a parameter regime very similar to that in a future collider.

Analytical expressions of the instability growth rate for the trailing bunches have been derived in Refs. [3, 4, 5, 6]. In a simple linear treatment, for small amplitudes ($y \ll \sigma_y$) an initial vertical perturbation of magnitude $\hat{y}$ is found to increase quasi-exponentially as [3]

$$y \approx \hat{y} \, \frac{1}{2\sqrt{2\pi}(t/\tau_c)^{1/4}} \, \exp(\sqrt{t/\tau_c}) \qquad \text{with} \qquad \frac{1}{\tau_c} \equiv \frac{4d_{gas}\sigma_{ion}\beta N_b^{3/2}n_b^2 r_e r_p^{1/2} L_{sep}^{1/2} c}{\sqrt{3} \, 3\gamma\sigma_y^{3/2}(\sigma_x + \sigma_y)^{3/2}A^{1/2}}, \qquad (1)$$

where $d_{gas} = p/(kT)$ denotes the residual gas density, σ_{ion} the cross section for collisional ionization, β the average vertical beta function, N_b the bunch population, n_b the number of bunches in the train, L_{sep} the bunch spacing (in meters), σ_x and σ_y the horizontal and vertical beam size, respectively, γ the beam energy in units of the rest energy, A the ion mass as a multiple of the proton mass, r_e ($= 2.8 \times 10^{-15}$ m) the classical electron radius, r_p ($= 1.4 \times 10^{-18}$ m) the classical proton radius, and c the speed of light. In the following, I will assume an ionization cross section $\sigma_{ion} \approx 2$ Mbarn and an atomic mass $A = 28$, i.e., nitrogen or carbon monoxide molecules.

The dependence of the vertical ion oscillation frequency on the horizontal position and the variation of the ion frequency along the beam line both lead to a decoherence of the beam-ion motion. If this decoherence is included in the analytical derivation, instead of Eq. (1) we expect an exponential growth [4, 5]:

$$y \approx \hat{y} \exp(t/\tau_e) \qquad \text{with} \qquad \frac{1}{\tau_e} \approx \frac{1}{\tau_c} \frac{c}{2\sqrt{2}l_{train}a_{bt}\omega_i} \qquad (2)$$

where l_{train} is the length of the train, $\omega_i \equiv c\left(\frac{4QN_b r_p}{3AL_{sep}\sigma_y(\sigma_x+\sigma_y)}\right)^{\frac{1}{2}}$ the coherent ion oscillation frequency, and a_{bt} the relative ion-frequency beat ($a_{bt} \approx 0.1$) due to the variation of the beam sizes along the beam line. Equation (2) still only applies to small-amplitude motion ($y \ll \sigma_y$).

In Ref. [6] Heifets showed that in the opposite regime of large oscillation amplitudes ($y \gg \sigma_y$) the amplitude growth is linear in time:

$$y \sim \sigma_y t/\tau_H \qquad \text{with} \qquad \frac{1}{\tau_H} \approx \frac{1}{\tau_c} \frac{c}{\tilde{\omega}_{ion}L_{sep}n_b^{3/2}} \qquad (3)$$

quantity	scenario I	scenario II
pressure p	100 ntorr	10 ntorr
temperature T	300 K	300 K
beam energy E	1.5 GeV	1.5 GeV
number of bunches / train n_b	20	20
bunch population N_b	2×10^{10}	5×10^9
hor. rms beam size σ_x	83 μm	83 μm
vert. rms beam size σ_y	5 μm	10 μm
trapping condition $L_{sep}\omega_i/c$	1.7	0.62
tune shift along train ΔQ_y	0.008	0.0001
linear rise time τ_c	147 ns	37 μs
rise time incl. decoherence τ_e	**1.4 μs**	**100 μs**
nonlinear rise time τ_H	22 μs	1.7 ms
simulated rise time	100 ns	25 μs

Table 1: Estimated FBII rise times for two different scenarios.

The FBII can only arise when the ions are trapped between bunches. Using the coherent ion frequency ω_i defined above, the trapping condition is written as:

$$L_{sep}\omega_i \leq 3.3\ c \tag{4}$$

For the ATF design parameters, this condition is fulfilled and, thus, the ions are trapped within a single bunch train. However, the ions will be lost in the 60-ns long gap between different trains.

Exemplary parameters and rise-time estimates in the ATF DR are listed in Table 1, considering 2 different scenarios. The first scenario assumes the present (March 97) average pressure of about 100 ntorr, the design emittances ($\gamma\epsilon_y = 30$ nm, $\gamma\epsilon_x = 4.3$ μm), the design beam sizes ($\sigma_x \approx 83$ μm, $\sigma_y \approx 5$ μm), and the maximum current per bunch ($N_b \approx 2 \times 10^{10}$). This combination of parameters represents a 'worst' case, with the fastest possible growth rate. In the second scenario, I assume an improved pressure of 10 ntorr, a degraded vertical emittance that is 4 times larger than the design value (i.e., $\gamma\epsilon_y = 120$ nm) and a bunch population of only $N_b = 5 \times 10^9$.

For these two sets of conditions, the analytical estimates of the e-folding rise time at small amplitudes ($y \leq \sigma_y$) vary between 1.4 μs (scenario I) and 100 μs (scenario II). Even in the latter case, the instability is still very fast and should be clearly observable.

In order to confirm the analytical estimates, I performed a few simplified computer simulations, in which every bunch as well as the ions generated over a certain distance were both represented by a single macroparticle, and the product of the two transverse beam sizes $\sigma_x \times \sigma_y$ was assumed to be constant. Initially, all bunches were randomly displaced by up to $\pm 10^{-4}$ σ_y. The motion of bunches and ions was then tracked for several thousand turns. Typical simulation results are displayed in Fig. 1. The simulated e-folding rise times of 100 ns and 25 μs, respectively, are consistent with the simple linear theory, which—without decoherence—predicts an instantaneous e-folding time of $\tau_{e,\ \text{lin}}(t) \approx 2\sqrt{\tau_c t}$. Because the simulation did not include any decoherence mechanism, the simulated e-folding times are about 3–10 times shorter than the expected e-folding times τ_e calculated from
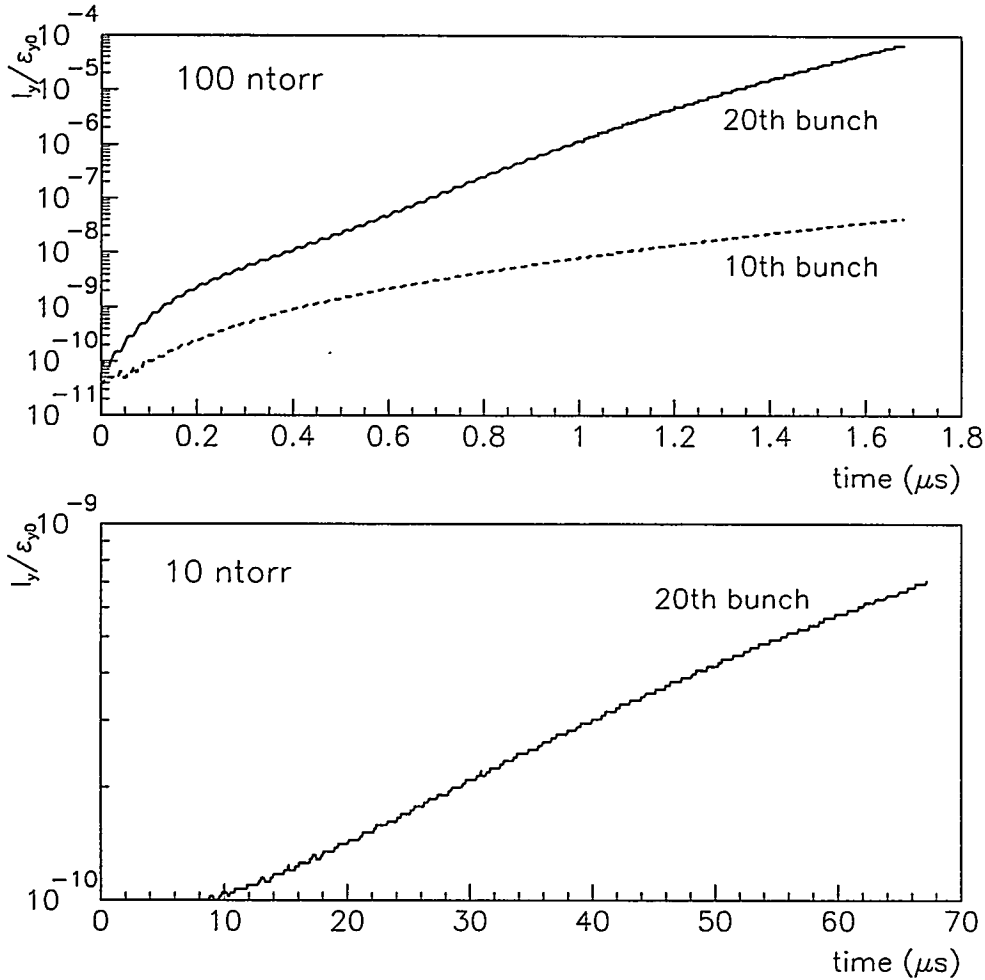
Eq. (2) and listed in Table 1,

Figure 1: Amplitude growth caused by FBII; top: scenario I, bottom: scenario II. The effective e-folding time for the 20th bunch is $\sim$100 ns and $\sim$25 μs, respectively.

In conclusion, as the ATF approaches its design parameters, the FBII will most likely be one of the predominant performance-limiting effects. At the moment no theory exists which would predict the emittance blow-up due to the FBII in the stationary state. Based on the ALS experiments one could expect an increase by a factor 2–4. However, since the predicted rise times in the ATF are much shorter than those in the ALS, there is no good justification for such an extrapolation. The ATF thus provides a unique possibility to study the FBII in a regime hitherto unexplored and of great interest for many future machines. If necessary, the instability rise time could be lowered by introducing additional gaps in the bunch train, by an improved vacuum pressure and/or by a dedicated fast bunch-by-bunch feedback system.

4

2.2 Head-Tail Ion Effect

At every point s along the ring at which the slope of the vertical dispersion is nonzero there is a correlation between the vertical displacement of a particle and its longitudinal position with respect to the bunch center, z, of the form

$$y_0(z,s) = \hat{y} z/\sigma_z \; \cos(\omega_\beta s/c + \phi_0) \tag{5}$$

where $\hat{y} = \eta'_y \sigma_y^2/\sigma_z$ describes the strength of the correlation, and ω_β is the betatron wave number. Equation (5) is a direct consequence of the symplecticity of the beam transport matrices [10]. Supposing that the residual vertical dispersion is dominated by a vertical kick at a single point in the ring, for every full revolution between two kicks the first-order dispersion is proportional to a pure betatron oscillation, and the ions generated by the head of the bunch excite the bunch tail in resonance. The resonant emittance growth over one turn is [11]:

$$\Delta\epsilon_y^{(1 \text{ turn})} \approx \frac{1}{2\pi\beta} \left(\frac{\hat{y} C \beta \lambda_{ion} r_e}{2\gamma \sigma_y (\sigma_x + \sigma_y)} \right)^2 \tag{6}$$

where λ_{ion} (m)$^{-1} \approx 6Np(\text{Torr})$ denotes the ion density at the end of the bunch, β the average beta function and C the ring circumference. Since the betatron tune is fractional, we may assume that the kicks experienced at different turns add incoherently. In this case, the emittance increases linearly with the turn number and the emittance growth rate is:

$$\frac{\Delta(\gamma\epsilon_y)}{\Delta t} \approx f_{rev}\gamma \; \Delta\epsilon_y^{(1 \text{ turn})} = \frac{\gamma f_{rev}}{2\pi\beta} \left(\frac{\eta'_y \sigma_y C \beta \lambda_{ion} r_e}{2\gamma \sigma_z (\sigma_x + \sigma_y)} \right)^2, \tag{7}$$

where f_{rev} denotes the revolution frequency (2 MHz). Using $\sigma_x \approx 88$ μm, $\sigma_y \approx 5$ μm, $\sigma_z \approx 5$ mm, $C \approx 150$ m, $\beta \approx 4$ m, $\gamma \approx 3000$, $\lambda_{ion}(\text{m}^{-1}) \approx 5 \, N_b \, p$ (torr), $N_b \approx 2 \times 10^{10}$, I find

$$\frac{\Delta(\gamma\epsilon_y)}{\Delta t} \approx 1.5 \times 10^{-13} \; \eta'_y{}^2 \left(\frac{p}{100 \text{ ntorr}} \right)^2 \; \text{m s}^{-1}. \tag{8}$$

For $\eta'_y \approx 0.1$ rad, the vertical emittance growth caused by the head-tail effect, Eq. (8), is 12 orders of magnitude smaller than the (horizontal) emittance growth due to quantum fluctuations,

$$\frac{\Delta(\gamma\epsilon_x)}{\Delta t} \bigg|_q \approx \frac{2\gamma\epsilon_{x0}}{\tau_x} \approx 1.2 \times 10^{-3} \; \text{m s}^{-1}, \tag{9}$$

where τ_x ($\tau_x \approx 7$ ms) denotes the horizontal damping time and $\gamma\epsilon_{x0}$ ($\gamma\epsilon_{x0} \approx 4$ μm) the horizontal equilibrium emittance. Therefore, as long as the slope of the vertical dispersion is the only source of y-z-correlation in the bunch, the head-tail ion effect appears to be negligibly small.

3 Emittance Growth in the Beam-Transport Line

3.1 Coherent Synchrotron Radiation

For intense short bunches, coherent synchrotron radiation (CSR) can lead to an enhanced energy spread and increased emittance growth. The effect of coherent synchrotron radiation has recently

been studied by various authors [12, 13, 14, 15]. Here, I will estimate the emittance growth caused by CSR in the beam-transport line (BT), which connects the linac and the damping ring.

The beam transport line comprises 6 vertical and 9 horizontal bending magnets. In each of these bending magnets the beam may radiate coherently. The CSR would be most significant for the highest design charge (bunch population $N_b = 2 \times 10^{10}$) and shortest possible bunch length ($\Delta z_{FWHM}/c \approx 10$ ps or $\sigma_z \approx 1.1$ mm). Table 2 presents other beam and magnet parameters.

parameter	value
rms bunch length σ_z	1.1 mm
rms energy spread σ_e	0.3%
hor. emittance $\gamma\epsilon_x$	3×10^{-4} m
vert. emittance $\gamma\epsilon_y$	3×10^{-4} m
bunch population N_b	2×10^{10}
length of hor. bend L_x	1.45 m
length of vert. bend L_y	1.00 m
hor. bending radius ρ_x	4.15 m
vert. bending radius ρ_y	4.20 m
rms hor. beam size σ_x	630 μm
rms vert. beam size σ_y	630 μm
average hor. beta function β_x	~ 4 m
average vert. beta function β_y	~ 4 m

Table 2: Some parameters assumed for the study of CSR effects in the ATF BT line.

The rms energy spread induced by CSR in free space was estimated for a Gaussian bunch on a circular orbit in Ref. [12]:

$$\Delta\sigma_\delta \approx 0.2 \, \frac{N_b r_e L_{dip}}{\gamma \rho^{2/3} \sigma_z^{4./3}} \tag{10}$$

where L_{dip} denotes the length of the bending magnet, r_e the classical electron radius, N_b the bunch population, ρ the bending radius, and σ_z the rms bunch length. The additional energy spread $\Delta\sigma_\delta^{(x)}$ ($\Delta\sigma_\delta^{(y)}$) induced in a horizontal (vertical) bend of the BT is 1.8×10^{-5} (1.3×10^{-5}). In the same way as its incoherent counterpart, coherent radiation results in emittance growth whenever it occurs at a position of nonzero dispersion and/or nonzero slope of dispersion.

Equation (10) describes a worst case, since it does not include the shielding effect of the vacuum chamber, which suppresses the CSR when the beam-pipe dimension is small or the bunch length large. In a horizontal bending magnet the shielding is important if [12, 16]

$$\sigma_z \geq \sqrt{\frac{h^2 w}{\pi^2 \rho}} \tag{11}$$

where h and w denote the full height and width of the vacuum chamber. In case of the ATF, $w \approx h \approx 24$ mm, $\rho \approx 4$ m, and the shielding is significant for bunch lengths $\sigma_z \geq 600$ μm. For an rms bunch length of 1.1 mm, the effect of CSR should be greatly suppressed.

Nevertheless, to obtain an upper bound on the emittance increase due to CSR, I have performed tracking simulations using a modified version of the program MAD [17, 18] which neglects shielding effects. In these simulations, at the center of each bending magnet the energy of a particle is varied as a function of its longitudinal position, based on the overtake 'wake' function derived in Ref. [12].

The simulation shows that, for the nominal parameters of Table 2 and without shielding, the normalized emittance would increase by an absolute value of 1.8×10^{-7} m horizontally and by 1.2×10^{-8} m vertically. This corresponds to an emittance growth of

$$\Delta(\gamma\epsilon_x) \approx 1.1 \times 10^{-5} \text{ m}$$
$$\Delta(\gamma\epsilon_y) \approx 2.6 \times 10^{-6} \text{ m} \tag{12}$$

to be added in quadrature to the incoming emittance of 3×10^{-4} m. [2]

In conclusion, even under fairly pessimistic assumptions on bunch length, bunch charge and shielding, the emittance growth due to coherent synchrotron radiation in the BT is insignificant.

3.2   Head-Tail Ion Effect

A perturbation of the same form as in Eq. (5) but with a much larger correlation amplitude $\hat{y}$, is induced by wake fields and accelerating rf voltage in the linac combined with (mismatched) horizontal or vertical dispersion in the BT. In the same manner as in the damping ring, ions generated at the bunch head can resonantly excite the bunch tail. The emittance increase after a distance L is obtained from Eq. (6) by replacing the circumference C with the distance L. With $\beta \approx 4$ m, $p \approx 100$ nTorr, $L \approx 80$ m, $\sigma_x \approx \sigma_y \approx 600$ μm, and $\lambda_{ion} \approx 10^4$ m^{-1}, I find

$$\Delta(\gamma\epsilon_{x,y}) \approx 5 \times 10^{-10} \left(\frac{\hat{y}}{\text{m}}\right)^2 \text{ m} \tag{13}$$

which for any realistic value of $\hat{y}$ (i.e., $\hat{y} < \sigma_y$) is quite negligible.

4   Emittance Growth in the Injector Linac

4.1   Quadrupole Wake

If a beam possesses a transverse quadrupole moment relative to the accelerator pipe axis, e.g., if the beam is not round or off axis, a quadrupole wake is generated. Although typically much weaker than the dipole wake, the quadrupole wake may not always be neglected. Quadrupole wake fields in linacs were discussed by Chao and Cooper in Ref. [19].

Two types of quadrupole moments exist: a normal quadrupole moment $Q_{q,1}$ and a skew quadrupole moment $Q_{q,2}$, which are defined by

$$Q_{q,1} = <x^2> - <y^2> \tag{14}$$
$$Q_{q,2} = 2<xy> \tag{15}$$

---

[2]I only tracked through 6 out of the 9 horizontal bends (and through all 4 vertical bends) and multiplied the resulting horizontal emittance growth by a factor of 1.5, to estimate the effect of the other three bends.

The wake field generated by a slice with quadrupole moments $Q_{q,1}$ and $Q_{q,2}$ gives rise to a Lorentz force on another slice following a distance z behind it [19], which reads

$$e\left(\vec{E} + \frac{\vec{v}}{c} \times \vec{B}\right) = e^2 W(z)\left[Q_{q,1}(x\hat{x} - y\hat{y}) + Q_{q,2}(y\hat{x} + x\hat{y})\right] \tag{16}$$

where $W(z)$ is the quadrupole wake function, and $\hat{x}$ and $\hat{y}$ denote unit vectors in the horizontal and vertical direction.

The significance of the quadrupole wake field in the ATF injector linac can be judged from the betatron phase shift that it induces along the bunch. To obtain a rough estimate, I consider a two-particle model, where each particle carries half the bunch charge, and the two particles are separated longitudinally by $\sim 1\,\sigma_z$. If the beam is injected on axis, the quadrupole moment at location s arises only from the beam-size variation, $Q_{q,1}(s) = \sigma_x(s)^2 - \sigma_y(s)^2$, and the phase shift of the 2nd bunch can be expressed by an integral over the linac length L,

$$\Delta\Phi_x \approx \int_0^L \frac{r_e W N_b}{4\gamma(s)}\,\beta_x(s)(\sigma_x(s)^2 - \sigma_y(s)^2)\,ds \tag{17}$$

In the ATF injector linac, the beta function scales roughly with energy, $\beta_x(s) \sim \gamma(s)$, and the beam sizes are, to first approximation, constant and independent of position. Ignoring the relative oscillations of σ_x and σ_y (which will reduce the effect of the quadrupole wake), I obtain a worst-case estimate:

$$\Delta\Phi_x \approx \frac{r_e W(\sigma_z) N_b \beta_{x,0}}{4\gamma_0}\,|\sigma_x^2 - \sigma_y^2|L \tag{18}$$

where β_{x0} denotes the initial beta function, γ_0 the initial Lorentz factor ($\gamma_0 \approx 160$), and $W(\sigma_z)$ the quadrupole wake function at a distance of $1\,\sigma_z$.

For the ATF structures the quadrupole wake function $W(\sigma_z)$ has not been calculated, but I can estimate its size by scaling from the dipole wake function, which at $1\,\sigma_z$ is about 1.2×10^{16} V/m/C per 3-m S-band structure. Dividing this value by the square of the iris radius (~ 10 mm) and converting to Gaussian units yields the estimate $W \approx 10^{10}$ m^{-5} for the quadrupole wake function per unit length in the ATF linac. This is not too different from (and about two times higher than) the number for the SLAC linac quoted in Ref. [19]. With this wake function and using $\beta_{x0} \approx 9$ m, $N_b \approx 2 \times 10^{10}$, $L \approx 80$ m, and $|\sigma_x^2 - \sigma_y^2| \approx 2$ mm^2, the phase shift between the two particles at the end of the linac is

$$\Delta\Phi_x \approx 2 \text{ rad}, \tag{19}$$

which is not insignificant. In Eq. (19), I have overestimated the quadrupole-wake effect for the perfect design lattice by neglecting some cancellations due to the oscillatory character of the two beam-size envelopes σ_x and σ_y. Regardless, the size of my estimate indicates that the emittance growth in the linac will be sensitive to the incoming beam parameters and that, in particular, the quadrupole wake fields caused by steering and matching errors into the linac can be important.

Since the quadrupole wake field introduces a coupling of the horizontal and vertical centroid betatron motion, via the induced quadrupole moment, the magnitude of this wake field can be measured by detecting the change of the vertical betatron phase advance as a function of a horizontal oscillation amplitude.

8

To explore the possibility of a quadrupole wake measurement in the ATF linac, I have performed computer simulations using the latest version of the code LIAR [20], which includes the short-range quadrupole wake field. For these simulations, I have chosen a bunch population of $N_b \approx 10^{10}$, a bunch length $\sigma_z \approx 5$ mm, horizontal and vertical normalized emittances of 3×10^{-4} m and an energy spread $\delta_{rms} \approx 1\%$. The beta function at the point of the initial energy 80 MeV is 1.93 m in both planes. I assumed the calculated quadrupole wake function for the SLAC S-band linac, although, according to the above scaling from the dipole wake function, the ATF wake field may be twice as strong. Further, a bunch was split into 20 slices and 3 macroparticles per slice were tracked through a model of the ATF linac.

Figure 2 presents a typical simulation result. It shows how the vertical orbit corresponding to a betatron oscillation of 500 μm initial amplitude is affected by a 4-mm horizontal oscillation. At the end of the linac, the difference is quite dramatic. Without quadrupole wake field, the vertical orbit would be independent of the horizontal position. As a cross check, this was also confirmed in the simulation.
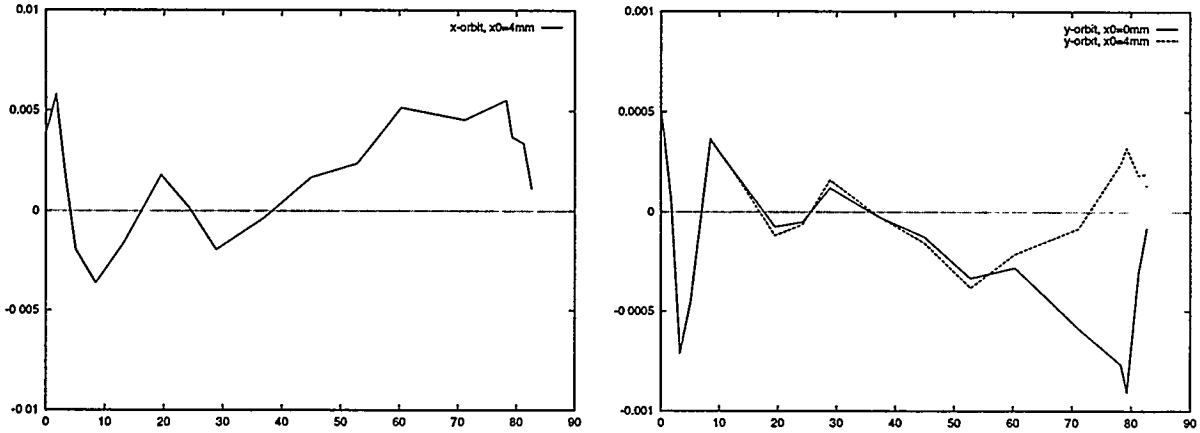

Figure 2: Simulation of a horizontal betatron oscillation in the ATF linac (top) and its effect on a small vertical oscillation (bottom), due to the quadrupole wake. The horizontal axis refers to the longitudinal position (in meters); the vertical axis gives the transverse coordinate (also in meters).

Since the quadrupole-wake effect shown in Fig. 2 is quite large and should be detectable, a first attempt has been made to measure it in the real ATF linac. At the time of this measurement, the bunch population was about $N_b \approx 6 \times 10^9$ at the entrance to the BT, and the rms bunch length about 5 mm. The measurement proceeded in complete analogy to the above simulations. The horizontal orbit was changed by exciting the steering coil ZH2L ± 1 (-1.5) A, generating a horizontal oscillation with an amplitude of about 3 mm, and the effect of this oscillation on the vertical betatron motion was studied by launching a vertical test oscillation with an initial amplitude of 600 μm. The vertical oscillation was generated with the vertical corrector ZV2, whose strength was increased by 0.1 A. For each horizontal corrector setting, 5-pulse average orbits were measured with and without excitation of the vertical corrector. The difference orbit for the two corrector settings is a vertical betatron oscillation, whose dependence on the horizontal orbit is the object of interest.

A preliminary first measurement result is depicted in Fig. 3. As expected, the vertical orbit

9

changes with the horizontal corrector setting. Unfortunately, the error of this measurement is comparable to the observed effect. This is indicated by the last figure showing a difference orbit for nominally identical conditions, which is as large as 200 μm. This nonreproducibility could be due to corrector hysteresis, to changes in the upstream orbit, or to bad pulses and BPM multiplexing. More measurements are required to confirm that the observed variation is due to a quadrupole wake field. The measurement could be improved by recording a larger number of orbits, by filtering bad BPM readings (i.e., those with low intensity numbers), or by generating still larger betatron oscillations.
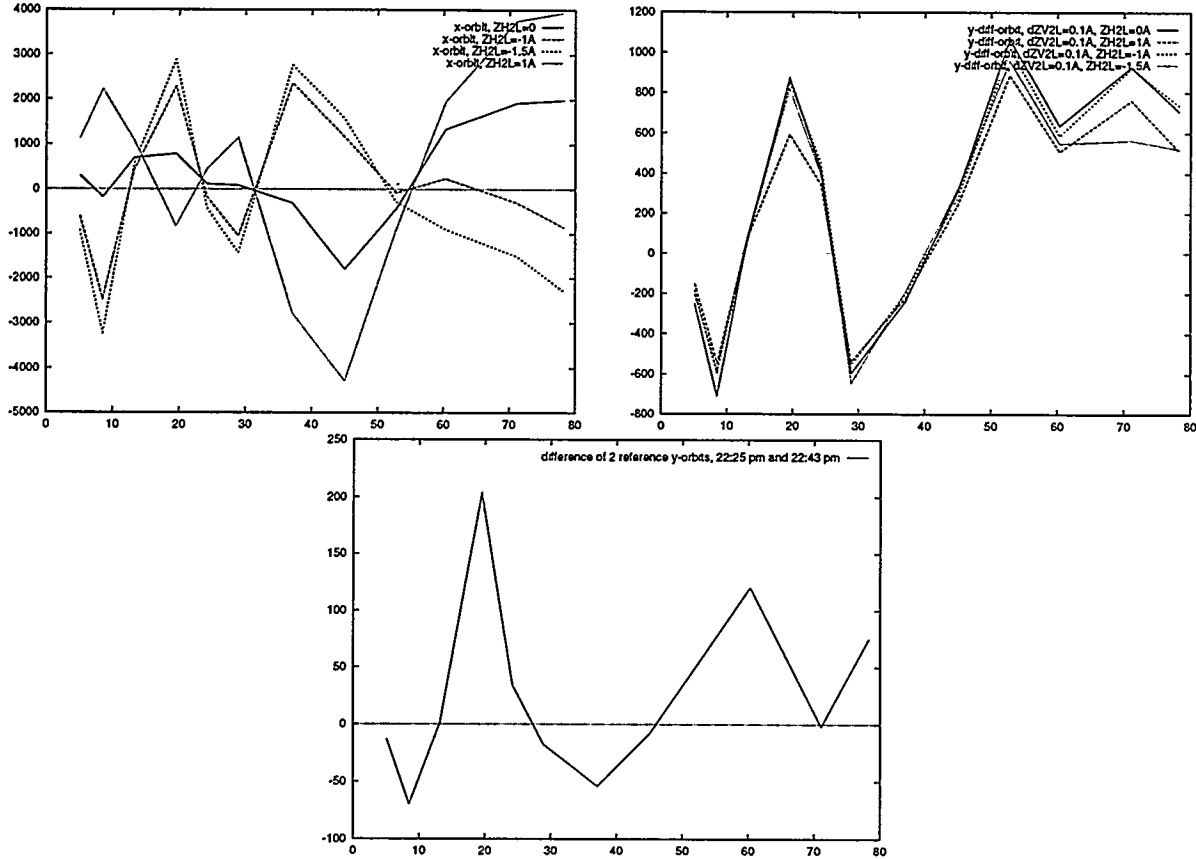

Figure 3: First attempt to measure the quadrupole wake field in the ATF linac: (top left) horizontal betatron oscillations, (top right) their effect on a vertical betatron oscillation, and (bottom) difference of two vertical orbits taken 20 minutes apart, under identical conditions. Horizontal axis is the longitudinal position (in meters) along the linac; vertical axis gives the horizontal or vertical beam position (in μm).

subsystem	process	effect & comment
DR	FBII	very fast rise time $\tau_e \approx 1\text{--}100~\mu s$
	head-tail ion effect	insignificant
BT	CSR	$\Delta\epsilon_y < 0.1~\%$, insignificant
	head-tail ion effect	insignificant
Linac	quadrupole wake	head-tail phase shift $|\Delta\Phi_{x,y}| \approx 2$ rad

Table 3: Various emittance-growth mechanisms in the different ATF subsystems.

5 Summary and Conclusions

In this note, I have studied several mechanisms which could cause emittance growth in the different ATF subsystems. Table 3 presents a concise summary of my results. I found that the performance of the ATF damping ring will likely be limited by a multi-bunch fast beam-ion instability (FBII). The resulting emittance growth is hard to predict, but based on the ALS experiments at least a doubling of the equilibrium emittance can be expected. The ATF offers the unique possibility to test, under realistic conditions, different countermeasures which have been proposed to cure or alleviate this instability.

In addition, quadrupole wake fields in the ATF linac were shown to be potentially important, both analytically and in computer simulations. A preliminary test measurement on the real machine provided some evidence of the quadrupole wake, although the measurement error appeared to be comparable to the effect observed. For a more precise determination. further refined studies will be needed. These may well result in the first measurement ever of a quadrupole wake field in an accelerator.

I have not uncovered any significant single-bunch head-tail ion effects, and, finally, I have determined that, even under the 'worst' possible conditions, the emittance growth due to coherent synchrotron radiation in the beam-transport line is too small to be measured.

Acknowledgements

References

[1] T. Raubenheimer et al., "The Vertical Emittance in the ATF Damping Ring", Nucl. Instr. Methods A335, p. 1 (1992).

[2] T. Raubenheimer, "Emittance Growth due to Beam Gas Scattering", KEK 92-7 (1992).

[3] T.O. Raubenheimer and F. Zimmermann, "Fast Beam Ion Instability, I: Linear Theory and Simulations", Phys. Rev. E 52, no. 5, p. 5487 (1995).

[4] G.V. Stupakov, T.O. Raubenheimer and F. Zimmermann, "Fast Beam Ion Instability, II: Effect of Ion Decoherence", Phys. Rev. E 52, no. 5, p. 5499 (1995).

[5] G.V. Stupakov, Proc. of Int. Workshop on Collective Effects and Impedance for B factories (CEIBA95), KEK Proceedings 96-6, p. 243 (1996).

[6] S. Heifets, Proc. of Int. Workshop on Collective Effects and Impedance for B factories (CEIBA95), KEK Proceedings 96-6, p. 270 (1996).

[7] F. Zimmermann, T.O. Raubenheimer, G. Stupakov, Proc. of IEEE PAC95, Dallas, p. 3102 (1995).

[8] J. Byrd, A. Chao, S. Heifets, M. Minty, T. Raubenheimer, J. Seeman, G. Stupakov, J. Thomson, F. Zimmermann, "First Observations of a 'Fast Beam-Ion Instability' ", submitted to Physical Review Letters (1997).

[9] S. Kurokawa, private communication (1997).

[10] K. Oide, private commuication (1997).

[11] P. Emma, T. Raubenheimer, F. Zimmermann, Proc. of 4th EPAC, London, p. 1162 (194).

[12] Ya.S. Derbenev, J. Rossbach, E.L. Saldin, and V.D. Shiltsev, "Microbunch Radiative Tail-Head Interaction", DESY TESLA-FEL 95-05 (1995).

[13] J.B. Murphy, S. Krinsky, R.L. Gluckstern, "Longitudinal Wake Field for an Electron Moving on a Circular Orbit", BNL-63090 (1996).

[14] E.L. Saldin, E.A. Schneidmiller, M.V. Yurkov, "On the Coherent Radiation of an Electron Bunch Moving in an Arc of a Circle", DESY TESLA-FEL 96-14 (1996).

[15] Ya.S. Derbenev and V.D. Shiltsev, "Transverse Effects of Microbunch Radiative Interaction", SLAC-PUB-7181 (1996).

[16] R.L. Warnock, "Shielded Coherent Synchrotron Radiation and Its Possible Effect in the Next Linear Collider", Proc. IEEE PAC 1991 San Francisco and SLAC-PUB-5523 (1991).

[17] H. Grote and C. Iselin, CERN Report No. CERN/SL/90-13 (1990).

[18] T. Raubenheimer, private communication (1995).

[19] A.W. Chao and R.K. Cooper, "Transverse Quadrupole Wake Field Effects in High Intensity Linacs", Particle Accelerators 13, p. 1 (1983).

[20] R. Assmann, C. Adolphsen, K. Bane, P. Emma, T. Raubenheimer, R. Siemann, K. Thompson, F. Zimmermann, "LIAR – A Computer Program for Linear Accelerator Simulations", version 1.8 (1997).